Volume 10:1-11

UJEMI+

The Undergraduate Journal of Experimental Microbiology & Immunology (+Peer Reviewed)

Engineering *Bordetella pertussis* BrkA Autotransporter for Chitin-Binding Domain Surface Expression: Exploring its Potential for Whole-Cell Immobilization

Alisa Li, Tiffany Wu, Karen Yeung, Alicia Zhang

Department of Microbiology and Immunology, University of British Columbia, Vancouver, British Columbia, Canada

SUMMARY The BrkA autotransporter is an important virulence factor in *Bordetella pertussis* that confers serum resistance and mediates cell adherence. As it is self-secreting and only one protein needs to be manipulated, this makes it a relatively simple secretion pathway that can be exploited to deliver proteins to the surface for applications such as whole-cell immobilization in fermentation bioreactors. In this context, the chitin-binding domain derived from *Pseudomonas aeruginosa* PAO1 chitinase C emerges as a promising candidate, given its strong affinity for chitin, an abundant polysaccharide, and its pH-sensitive characteristics that simplifies the process of retrieving cells after a bioreaction. As such, we aim to exploit the BrkA autotransporter secretion system to export the chitin-binding domain to the cell surface. By leveraging the binding properties of the chitin-binding domain to chitin, we also aim to explore its potential in whole-cell immobilization. In our study, we successfully engineered a recombinant plasmid (TAAK-A54) by substituting part of the BrkA passenger domain with the chitin-binding domain. A western blot indicated expression of the intracellular chitin-binding domain with a molecular weight of 52 kDa, and the extracellular processed form at 38 kDa. A trypsin accessibility assay confirmed the expression and export of the chitin-binding domain to the cell surface. Lastly, we observed through microscopy that *Escherichia coli* cells expressing the chitin-binding domain can interact with chitin. Samples had decreased turbidity following incubation with chitin resin, with a maximum 3-fold change relative to the negative control, suggesting that cells were able to be immobilized by chitin. This study enhances the understanding of the repertoire of heterologous proteins that the BrkA autotransporter system can secrete. We demonstrated the feasibility of leveraging the BrkA secretion system for the external presentation of the chitin-binding domain. Our results indicate that the chitin-binding domain is worthy of further study for applications in whole-cell immobilization.

Published Online: September 2024

Citation: Li, Wu, Yeung, Zhang. 2024. Engineering *Bordetella pertussis* BrkA autotransporter for chitin-binding domain surface expression: exploring its potential for whole-cell immobilization. UJEMI+ 10:1-11

Editor: Shruti Sandilya, University of British Columbia

Address correspondence to: https://jemi.microbiology.ubc.ca/

INTRODUCTION

Cell immobilization has various applications in bioremediation, waste management, biosensors in tissue regeneration, and biocatalytic reactors (1). For example, cell adsorption on inert surfaces such as silica gels is used to segregate and recover cells after a bioreaction is complete (2). Immobilized cells are useful since they can be repeatedly used without loss of their metabolic activities which can improve efficiency and cost-effectiveness. Microorganisms retained on a carrier can be used in continuous production processes since the biocatalyst does not need to be refilled. However, challenges have emerged concerning the stable retention of cells amid environmental perturbations, notably hydrodynamic shear forces. The advantages of using recombinant protein technology include strong and reversible binding of proteins to the support surface, mild adsorption conditions,

and the lack of diffusion constraints (3). Engineered cells have the potential to make a large environmental impact, especially for heavy metal pollution in industrial wastewater, one of the most critical environmental problems worldwide. Traditional biological treatment processes poorly remove hazardous compounds due to their toxicity. However, engineered cells can have a strong resistance to toxic chemicals and can be engineered to selectively bind to and remove heavy metal species from wastewater. Thus, many fusion tags have been studied for cell immobilization, such as the cellulose-binding domain, poly-histidine, and glutathione S-transferase (2). However, a relatively understudied yet promising tag is the chitin-binding domain (CBD).

Chitin is a long-chain polymer of N-acetylglucosamine, an amide derivative of glucose. Bacteria synthesize and secrete chitinases that catalyze the hydrolysis of chitin into chitodextrins. One example is the *Pseudomonas aeruginosa* PAO1 chitinase C (ChiC), a secreted chitinolytic enzyme involved in various carbohydrate metabolic processes including the hydrolysis of O-glycosyl compounds (4). ChiC is predicted to have three domains: a catalytic domain, a fibronectin-like type III domain, and a 47-amino acid CBD that helps ChiC bind to and degrade chitin (4). CBD is an appealing target for immobilization due to its strong affinity and specificity for chitin via hydrophobic interaction (5). Additionally, bound CBD offers the advantage of pH-dependent release, a simple and efficient method for cell retrieval post-immobilization. Chitin, being the most abundant natural polysaccharide found in fungal cell walls and invertebrate exoskeletons, ensures economic feasibility and aligns with sustainable practices, emphasizing the pragmatic and ecological appeal of CBD-based immobilization (2). As such, there have been many studies displaying the success of CBD-based immobilization of different proteins including β-glucosidase, β-galactosidase, and D-hydantoinase (6–8). Nonetheless, its applications in whole-cell immobilization are relatively unexplored.

One study showed the effectiveness of CBD in immobilizing Gram-positive bacteria, such as *Lactococcus lactis*, when fused with cell wall anchor proteins PrtP and AcmA (9). Another study engineered the CBD from chitinase A1 to the lipoprotein (Lpp)–OmpA fusion vehicle for cell immobilization (2). However, there have been no studies testing whole-cell immobilization using natural Gram-negative secretion systems such as type V autotransporters. Type V secretion systems are known for their simplicity and efficiency in surface protein expression because they rely on a single protein, the autotransporter, for self-secretion and anchoring to the cell surface (10). One example is the serum-resistance-killing protein A (BrkA) autotransporter, a crucial virulence factor in *Bordetella pertussis* that confers serum resistance and contributes to adherence to host cells (11). BrkA has a 42 amino acid signal peptide for cell membrane localization, a passenger domain responsible for the protein's effector functions, and a translocation unit, made of a short linker fused to the β-domain, that forms a channel to transport the passenger domain to the cell surface (12). Previous studies that substituted the passenger domain with various proteins including biocatalysts and single-chain antibodies have shown considerable success in protein export and the preservation of enzyme activity (13).

We hypothesize that the BrkA autotransporter can be engineered to secrete CBD to the cell surface and retain its chitin-binding activity for whole-cell immobilization on chitin. In this study, we designed a recombinant BrkA-6X histidine (6XHis)-CBD plasmid, confirmed CBD expression and export, and tested CBD-based whole-cell immobilization.

METHODS AND MATERIALS

Gene block design. A gene block was designed using SnapGene and the sequence was sent to Integrated DNA Technologies (IDT) for construction. The CBD region was based on the NCBI sequence of ChiC in *P. aeruginosa* PAO1 (NC_002516.2, 2530289 - 2531840) (4) from amino acids 436 to 482 (14). A GGGGS linker sequence was added to both sides of the CBD gene to maintain the post-translation functionality of the protein (15). A 6XHis tag was added to the 5' end of the CBD gene before the linker to detect BrkA-CBD recombinant protein expression and surface display through western blot analysis. Flanking the 6XHis-CBD gene sequence are homologous regions to the KAX5A plasmid 20 base pairs (bp) upstream and downstream of the StuI restriction site. KAX5A was generously provided by Rachel Fernandez (14). Two cytosines were added to the end of the 5' homologous region,

and a single guanidine was added to the beginning of the 3' homologous region to ensure in-frame insertion. Excluding the homologous regions, codons were modified throughout the gene block sequence to remove the StuI restriction site and to comply with IDT™ gene block GC content criteria by eliminating homopolymeric runs of six or more Gs and Cs, which effectively reduced the G/C content.

Overnight culture preparation. DH5α *E. coli* cells containing KAX5A or TAAK-A54 plasmid were grown in Luria Broth (LB) supplemented with ampicillin (100 μg/mL) overnight in a 37°C shaking incubator. Cultures were collected when optical densities at 600 nm (OD_{600}) reached 1.0 for plasmid isolation and incubation with chitin resin, and 1.5-2.0 for trypsin assay and protein extraction (Ultrospec 3000 Spectrophotometer).

KAX5A plasmid isolation. KAX5A plasmid from an overnight culture of DH5α *E. coli* cells containing the KAX5A plasmid (OD_{600} = 0.5-1.0) was isolated and purified using the EZ-10 Spin Column Plasmid DNA Miniprep Kit (Bio Basic) as per manufacturer instructions. Plasmid concentration was determined using the NanoDrop™ 2000. The purified plasmid was stored at -20°C.

Restriction Digestion of KAX5A. Restriction digest of KAX5A was performed with StuI according to GeneArt™ Gibson Assembly EX Cloning Kit (Invitrogen) manufacturer recommendation and ThermoFisher Scientific Eco147I product protocol. 30 units (U) of StuI were used to digest 2 μg of purified KAX5A plasmids in a 100 μL reaction. To verify digestion, restriction digest products were visualized on a 1% agarose gel stained with 1X SYBR Safe DNA gel stain (100V for 60 minutes) using the Bio-Rad® ChemiDoc™. The linearized KAX5A was used as the vector in Gibson assembly.

Gibson assembly of 6XHis-CBD gene block and KAX5A plasmid. Gibson assembly of 6XHis-CBD gene block and KAX5A plasmid vector was performed using the GeneArt™ Gibson Assembly EX Cloning Kit (Invitrogen) based on manufacturer protocol. The 10 μL reaction consisted of 1.19 μL of KAX5A plasmid vector (111.5 ng/μL), 1.24 μL of 6xHis-CBD gene block insert (5 ng/μL), 2.57 μl of deionized water, and 5 μL of Master Mix A. The reaction was incubated in the thermocycler with the following conditions: 37°C for 5 minutes, 75°C for 20 minutes, a decrease of 0.1°C/second until the temperature reached 60°C, 60°C for 30 minutes, and finally a decrease of 0.1°C/second until the temperature reached 4°C. Next, 10 μL of Master Mix B was added and the reaction was incubated at 45°C for 15 minutes. The final Gibson assembly product was subjected to StuI (Thermofisher Scientific) restriction digestion. The 45 μL reaction consisted of 2 μg Gibson assembly product, 5 μL 10X buffer B, 50 U of StuI, and 16 uL of nuclease-free water and was incubated at 37°C for one hour.

Transformation of DH5α *E. coli* cells. The final Gibson assembly product was transformed into commercially competent DH5α *E. coli* cells (Invitrogen) by the heat shock method described previously (http://cmdr.ubc.ca/bobh/method/cacl2-transformation-of-e-coli/). Transformed cells were plated on Luria agar supplemented with ampicillin (100 μg/mL) to select recombinant colonies. Overnight cultures of transformed cells were prepared with methods described previously.

TAAK-A54 Sequencing. TAAK-A54 plasmid from overnight culture of DH5α *E. coli* cells containing TAAK-A54 (OD_{600} = 1.0) was isolated and purified using the EZ-10 Spin Column Plasmid DNA Miniprep Kit (Bio Basic). The purified plasmid (59.4 ng/μL) was diluted to 30 ng/μL. 15 μL of the dilution was sent to Plasmidsaurus for sequencing.

Trypsin Accessibility Assay. Cells from overnight cultures (OD_{600} = 1.5-2.0) were harvested by centrifugation (12000 RPM for 2 minutes) and resuspended in 200 μL of phosphate-buffered saline (PBS). 4 μL of trypsin (10 mg/mL) was added to each tube and incubated for different time periods (10 minutes, 30 minutes, and 60 minutes) in the 37°C shaking incubator. Cells were further harvested and washed 4 times with 1X PBS. 100 μL of 2X

Laemmli sample buffer (Bio-Rad) and 5% β-mercaptoethanol (βME) were added to deactivate trypsin in TAAK-A54 and KAX5A samples and 5 µL was added to ChiC. Trypsin accessibility experiments were adopted and modified from (14).

Protein Extraction. Cells from overnight cultures (OD_{600} = 1.5-2.0) were harvested by centrifugation (12000 RPM for 2 minutes). Harvested cells were lysed in 100 µL of 2X Laemmli sample buffer (Bio-Rad) containing 5% βME and incubated at 95°C for 5 minutes. Proteins were isolated from cell lysates through centrifugation at 4°C for 30 minutes at 15000 RPM.

Western blotting. Isolated protein samples were subjected to Sodium dodecyl-sulfate polyacrylamide gel electrophoresis (SDS PAGE), transferred onto a nitrocellulose membrane (Bio-Rad), and stained with Ponceau S to verify equal loading and proper transfer. The membrane was blocked with 5% skim milk powder in 1% Tris-buffered saline with 0.1% Tween® 20 detergent (TBS-T) (10 mL) overnight at 4°C on an orbital shaker. This was followed by incubation with anti-histidine antibody (Invitrogen) (10 mL, 1:1000 dilution in 1% TBS-T) for one hour at room temperature and then incubation with HRP-conjugated goat anti-mouse IgG antibody (Invitrogen) (10 mL, 1:10000 dilution in 1% TBS-T) for one hour at room temperature. Chemiluminescence detection reagents (Bio-Rad Clarity Max Western ECL Substrate) were used 1:1 to detect protein bands with the ChemiDoc MP Imaging System (Bio-Rad).

OD_{600} assay of chitin beads and DH5α *E. coli* cells. 2 mL of chitin resin (NEB #S6651) was allowed to settle until a pellet was formed. The supernatant was then aspirated. The chitin bead bed was washed with 2 mL of 1X PBS and harvested by centrifugation (5000 RPM, 30 seconds) three times. The supernatant was aspirated, and the chitin bead bed was equilibrated in 2 mL LB supplemented with ampicillin (100 µg/mL). Overnight cell cultures were standardized to OD_{600} of approximately 1.00 and allotted to five 50 mL conical tubes. For each 2 mL of culture, 0 µL, 10 µL, 20 µL, 50 µL and 100 µL of washed chitin resin were added to each culture aliquot respectively. The mixture was incubated on a rotary orbiter at 150 RPM for 15 minutes at 4°C. Afterwards, mixtures were transferred to cuvettes (n = 1), and allowed to settle at 4°C for 15 hours. Images of cuvettes were captured with a digital camera before and after the incubation. Autoaggregation experiments were adopted and modified from (16)**.**

Staining of chitin beads and DH5α *E. coli* cells. At t = 22 h, 1 mL of cell culture and chitin resin mixture was pipetted into a microfuge tube. Chitin was allowed to settle until the chitin beads were pelleted, and the supernatant was removed. The remaining chitin bed volume was washed with 500 µL of 1X PBS and harvested by centrifugation (5000 RPM for 30 seconds) three times. Chitin was resuspended in 200 µL of 1X PBS and was allowed to settle until the chitin beads pelletted. 20 µL of settled chitin resin was pipetted onto a microscope slide and stained with 0.2 µL of Crystal Violet dye (17). The slide was visualized under a brightfield microscope with a 40X objective lens. Images were captured digitally.

RESULTS

The TAAK-A54 recombinant plasmid was engineered by inserting the CBD and a 6XHis tag into the KAX5A plasmid (Fig. 1A). The TAAK-A54 plasmid (Fig S1) was assembled through Gibson assembly. Insertion of the CBD and histidine tag occurred at the StuI restriction site located at alanine 54 of BrkA in the KAX5A plasmid. Nanopore sequencing was performed to confirm the proper assembly of the recombinant plasmid. Considering the type Va autotransporter secretion pathway mechanism (18) utilized by BrkA and the TAAK-A54 plasmid construct, the theoretical size of the BrkA-CBD recombinant protein located in the cytoplasm without modifications is 56.6 kDa (Fig 1B, S2). The intracellular protein located within the periplasm, post-N-terminal signal peptide cleavage, is predicted to be 52.0 kDa (Fig 1B, S2). The extracellular surface display protein, after both N-terminal signal peptide cleavage and β-domain cleavage, is predicted to be 21.5 kDa (Fig 1B, S2).

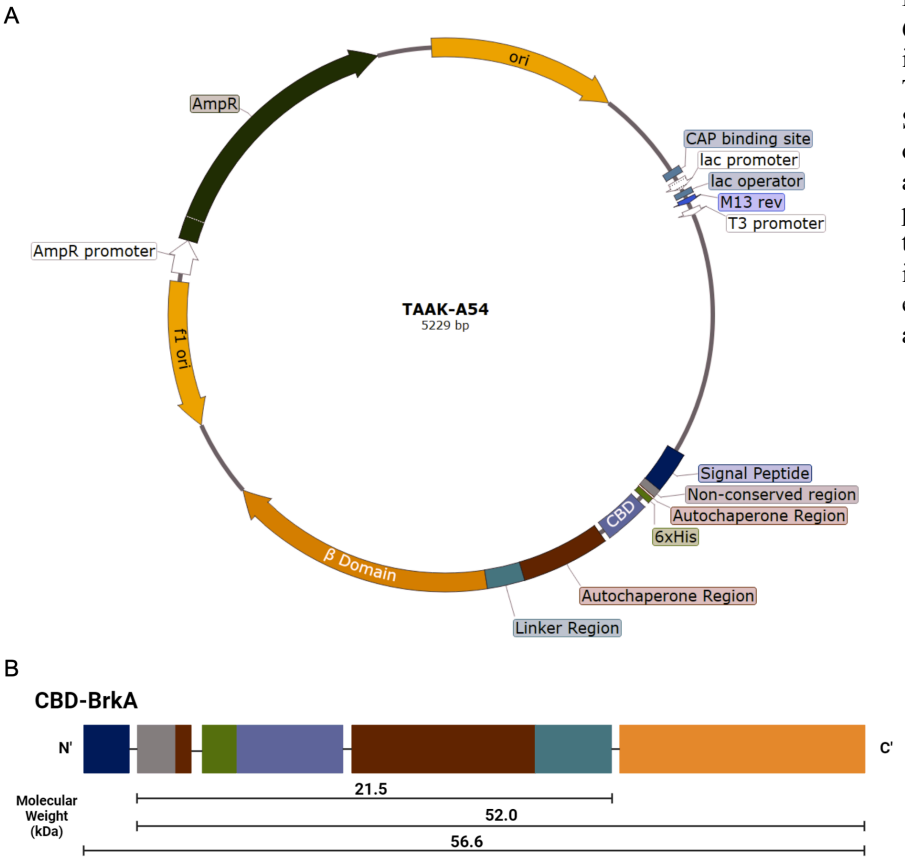

FIG. 1 TAAK-A54 plasmid design. A 6XHis tag and the CBD were inserted into the KAX5A plasmid. (A) Map of TAAK-A54 plasmid generated using Snapgene 6.2. (B) Protein domain map of recombinant BrkA-CBD. Domains are colour coded according to the plasmid map. The molecular weight of the entire protein (56.6 kDa), intracellular (52.0 kDa), and extracellular (21.5 kDa) conformations are highlighted.

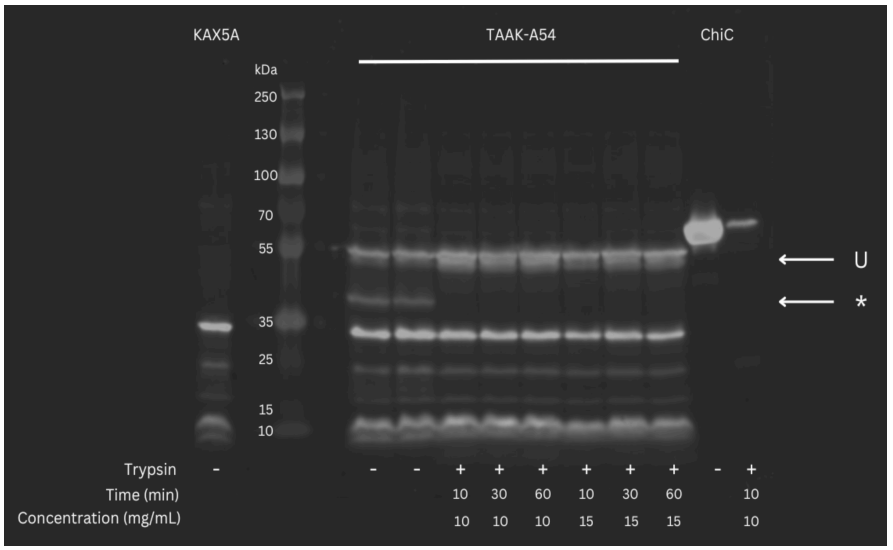

FIG. 2 BrkA-CBD is expressed and exported to the cell surface. Anti-6XHis-Tag Western blot against *E. coli* DH5α whole protein lysates was probed with anti-6XHis mouse and detected using goat anti-mouse horseradish peroxidase. Cells were processed in the presence (+) or absence (-) of trypsin as described in the methods. KAX5A is the wild-type BrkA vector negative control. Purified chitinase C from *P. aeruginosa* PAO1 was the positive control. The ruler used was PageRuler™ Plus Prestained Protein Ladder. 52 kDa is the unprocessed intracellular chitin-binding domain (U). 38 kDa is the processed extracellular CBD (*).

Chitin-binding domain was expressed and exported to the cell surface. To determine if CBD can be expressed, we conducted an anti-6XHis tag western blot on *E. coli* DH5α cells (Fig. 2). To determine if CBD can be processed and exported to the cell surface, we performed a trypsin accessibility assay in varying incubation times and concentrations. The expected 52 kDa intracellular CBD was observed in the presence and absence of trypsin. However, there was a slight double band in all samples, especially in the trypsin conditions. There was a 38 kDa band which was exported to the cell surface as shown by the disappearance of the band in all trypsin samples. Thus, this is likely the extracellular CBD. Time and concentration-dependent effects were not observed for the trypsin accessibility assay. No clear band with a molecular weight corresponding to the expected 21.5 kDa extracellular CBD was observed. Several bands below 35 kDa were observed in the negative control suggesting that they are

background signals. Based on these results, CBD can be expressed on TAAK-A54 and exported to the cell surface.

CBD-expressing cells can be immobilized by chitin beads. To study if CBD-expressing cells can be immobilized by chitin, we analyzed the settling profiles of cell cultures incubated with different concentrations of washed chitin resin by comparing OD_{600} readings before and after a 15-hour incubation period (Fig. 3). Given the higher densities of chitin beads compared to bacterial cells, the binding of suspended cells to these beads would result in reduced turbidity and OD_{600} readings. The OD_{600} of all cultures was normalized to 1.0 before chitin was added. As expected, the TAAK-A54 cultures exhibited lower turbidity after incubation with chitin resins than the KAX5A cultures, which do not express extracellular CBD (Fig. 3A). OD_{600} readings of the chitin-treated TAAK-A54 cultures also decreased more than that of their KAX5A counterparts (Fig. 3B). Furthermore, the change in OD_{600} readings of TAAK-A54 appeared to be dose-dependent, where higher concentrations of chitin resulted in increased bacterial aggregation (Fig. 3B). No statistical analysis was performed, as this experiment was performed with one replicate. Subsequent repeats of the experiment did not yield consistent results (Fig. S4). To visualize the interaction of CBD-expressing cells to chitin beads, chitin beads that had been incubated with cell culture for 22 hours were stained and viewed under a brightfield microscope at 400X magnification. Cultures were stained with crystal violet to ease visualization. Microscopic images revealed clusters of purple specks surrounding the chitin beads incubated with TAAK-A54, while far fewer purple specks were localized to the surface of the chitin beads incubated with KAX5A (Fig. 3C). Chitin beads (20 to 100 µm in diameter) are 20 to 100 times larger than bacterial cells, suggesting that the clusters of purple specks surrounding the chitin beads that had been incubated with TAAK-A54 cultures correspond to CBD-expressing cells bound to the chitin bead surface (Fig. 3C). Collectively, these results primarily suggest that CBD-expressing cells can bind to chitin. However, technical replicates should be performed in order to validate the efficacy of the OD_{600} readings of TAAK-A54 being dose-dependent.

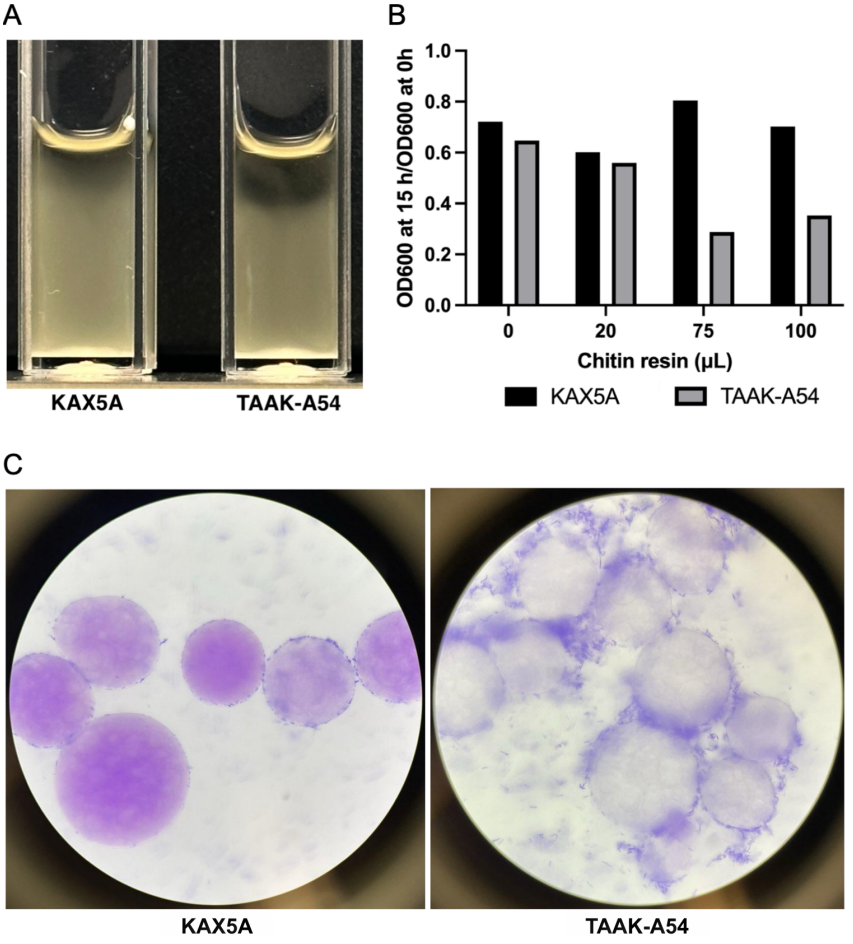

FIG. 3 BrkA-CBD-expressing cells bind to chitin beads. *E. coli* transformed with KAX5A (negative control) and TAAK-A54 (BrkA-CBD) plasmids were incubated with chitin resin (n = 1) at 4°C for 15 hours. Before incubation, OD_{600} of all samples were normalized to 1. (A) Representative image of 100 µL of chitin resin incubated in 2 mL of culture. (B) OD_{600} reading of cultures incubated with 0, 20, 75, and 100 µLs of chitin. (C) Microscope images of post-incubation cells (T = 22 hours) with chitin resins were stained with crystal violet and viewed under a bright-field microscope at 400X magnification.

DISCUSSION

Our study aimed to design a recombinant BrkA-CBD protein to determine whether BrkA can export CBD to the cell surface. We also assessed the potential of BrkA-CBD for whole-cell immobilization by testing the interaction between chitin and CBD-expressing cells. To achieve these aims, we designed the recombinant plasmid with Gibson assembly and confirmed the presence of the CBD insert via Nanopore sequencing. Then, we tested CBD expression and export with an anti-6XHis Western blot. Finally, we generated data that suggest that the CBD can immobilize whole cells with chitin resin.

The TAAK-A54 recombinant plasmid was engineered by designing a custom gene block comprising the CBD and a histidine tag and inserting it into the KAX5A plasmid within the autochaperone region of BrkA (Fig. 1). The KAX5A plasmid was selected as the vector because it is a modified form of BrkA, where the autochaperone region (Glu601-Ala692) is retained while most of the passenger domain is removed (Ala52-Phe600). The StuI restriction site, located within the autochaperone region, was selected as it was the only site closest to the BrkA N-terminal signal peptide sequence. However, this insertion could potentially impact protein export and folding because this region is necessary for proper protein folding (14). Our data indicate that this was not a major issue, although future studies can optimize for high cell-surface expression of CBD-BrkA by moving the CBD insertion site.

CBD was expressed in the TAAK-A54 plasmid (Fig. 2). In all TAAK-A54 samples, there was a band at 52 kDa that corresponds to our expected size of intracellular CBD. The persistence of these bands in the presence of trypsin confirms that it is an intracellular protein. There was a slight multiple-band effect observed for the 52 kDa bands in all samples. This may be attributed to excess protein content loaded onto the gel as our Ponceau stain indicated highly concentrated samples (Fig. S3). The effect is more prominent in the trypsin samples because they may have a relatively higher protein concentration since protein lysate volumes were not standardized. We relied on the Ponceau stain to assess equal protein loading; however, it provides only a rough estimation. Furthermore, the trypsin accessibility assay did not reveal a time or concentration-dependent effect. All TAAK-A54 samples incubated with trypsin exhibited a complete disappearance of the 38 kDa band. This suggests that a 10-minute incubation with 10 mg/mL of trypsin was likely more than sufficient to digest all extracellular proteins. Notably, the ChiC positive control showed a residual signal after trypsin digestion. As a secreted protein, ChiC is stable extracellularly, potentially concealing some protease sites (19). Moreover, the standard trypsin-to-protein ratio is 1:20 w/w (20). The positive control likely contained a higher protein concentration compared to the TAAK-A54 samples. Therefore, the incomplete digestion of the positive control was likely due to excess protein content and protein structure. While we were able to identify CBD signals in TAAK-A54 lanes, numerous non-specific background bands were observed in the Western blot (Fig. 2). Reducing the concentration of protein lysates or antibodies may alleviate non-specific binding, as demonstrated in previous studies (21). Given the high protein content in our experiment, this adjustment may yield improved results (Fig. S3).

Trypsin-digested samples indicate that the 38 kDa band likely corresponds to extracellular CBD (Fig. 2). The expected size for the processed and exported CBD is 21.5 kDa. We speculate that the observed size difference is due to the structure of CBD which may be preventing it from migrating at the same rate as the ladder. The presence of prolines, known to introduce kinks in proteins and slow down SDS-PAGE migration, could explain this phenomenon (22). The 22 prolines in ChiC would explain why the purified protein ran higher than expected. The expected size is 55 kDa but it is approximately 65 kDa compared to the ladder. Given that the CBD was derived from ChiC and it contains 4 prolines, there may be structural abnormalities in the processed CBD that cause it to migrate slower than the ladder thus, giving a higher molecular weight than expected. This possibility is supported by the example of the *B. pertussis* virulence factor pertactin. Due to its proline-rich regions, it can form a kink that is stable even in the presence of SDS and βME causing it to migrate higher than its expected size (11). Despite deviating from the expected size, we believe that the 38 kDa band is very likely to be extracellular CBD for various reasons. First, it is the only known protein with a histidine tag in the TAAK-A54 plasmid. Second, the absence of this band in the KAX5A negative control which has high background signals suggests its exclusive presence in our TAAK-A54 plasmid. Lastly, our functional assays suggest that cells were

able to bind to chitin resin, which would only be possible if CBD was exported to the cell surface.

All TAAK-A54 cultures that had incubated with different volumes of chitin resin had lower OD_{600} readings compared to their KAX5A counterparts, including the cultures without chitin (Fig. 3B). The OD_{600} of TAAK-A54 cultures also decreased as volumes of incubated chitin resin increased, suggesting that TAAK-A54 cells have bound to and settled with chitin beads (Fig. 3B). Apart from the dense chitin beads that had readily settled, a clear top layer had also separated from the turbid bottom layer in liquid cultures over time due to gravity. All TAAK-A54 cultures had similar portions of the cleared layer, regardless of the added chitin resin volume, but a significant OD_{600} drop was observed at higher chitin concentrations (Fig. 3B). This suggests that the depth of the cleared portion is not indicative of the chitin-binding ability of TAAK-A54 cells. Thus, we measured OD_{600} of our samples. To confirm that the decrease in OD_{600} was the result of CBD-expressing cells interacting with chitin beads rather than the intrinsic higher rate of TAAK-A54 settlement, the incubated cultures and chitin beads were stained to visualize the interaction. Many cells, stained purple, were observed around chitin beads incubated with TAAK-A54 but there were few stained cells around chitin beads incubated with KAX5A (Fig. 3c). The same results were observed after both samples were rinsed two extra times with PBS (data not shown). The results observed in these microscopic images resemble scanning electron microscopy (SEM) images which expressed the CBD with the Lpp-OmpA system for whole-cell immobilization (2). In both experiments, CBD-expressing cells were observed to have bound to the chitin beads (2). These data suggest that BrkA-CBD-expressing cells are capable of being bound to chitin through the CBD's interaction. Nonetheless, this experiment should be repeated with technical replicates for statistical analysis and reproducibility.

Although both KAX5A and TAAK-A54 plasmids were transformed into DH5α *E. coli* strains, cells transformed with TAAK-A54 settled faster than cells transformed with KAX5A (Fig. S5). Cell cultures with TAAK-A54 transformants also had a lower OD_{600} reading compared to KAX5A after a 15-hour incubation at 4°C (Fig. 3B). Given that the only differences between KAX5A and TAAK-A54 cultures are the plasmid and proteins that they are expressing, these observations suggest that TAAK-A54's expression of CBD is likely altering the settling rate of DH5α *E. coli* strains when left to sit. Previous studies found that the BrkA autochaperone region at Glu601-Ala692 mediates the proper folding of the BrkA passenger domain (14). The deletion of these amino acid residues may lead to aberrant protein misfolding, resulting in proteasomal degradation (14). Additionally, the OmpT protease, found at the cell surface, has been found to alter recombinant proteins (23). As our CBD was inserted within the autochaperone region of BrkA, this may have resulted in a partial denaturation of extracellular BrkA-CBD mediated by OmpT. This likely resulted in the non-uniform decrease in OD_{600} readings after TAAK-A54 cultures incubated with increasing volume of chitin (Fig. 3B). It is additionally possible that cell-surface BrkA-CBD could mediate intercellular interactions, which would cause the slight increase in aggregation of the TAAK-A54 cultures (14). If cells aggregate, these aggregate densities would increase and settle more rapidly than non-aggregated cells, and form cell clusters. This is likely what happened to our CBD-expressing cell cultures, as we observed clusters of CBD-expressing cells around chitin beads (Fig. 3C). Although the cultures were incubated at 4°C to minimize cell growth, cells would still replicate over time and cause turbidity and OD_{600} to increase. Since the two sets of cultures were transformed with different plasmids, these cultures might be replicating at different rates. If TAAK-A54 cells replicate slower than KAX5A cells, chitin-free TAAK-A54 will have a lower OD_{600} than chitin-free KAX5A after both cultures were left to sit – which parallels with the result of our experiment (Fig. 3B). As a result, all TAAK-A54 cultures had larger clear layer portions (Fig. 3A) and the chitin-free TAAK-A54 culture also had lower final OD_{600} readings compared to KAX5A (Fig. 3B).

In addition, cell-surface protein antigens can impact the expression of cell-surface proteins after subculturing (24). Overnight TAAK-A54 cultures used in the initial experiment (Fig. 3) were prepared from the initial plate and those in the subsequent experiment (Fig. S4) were prepared from a subculture of the initial plate. It is likely that subculturing had introduced surface protein modifications to TAAK-A54 cells, altered the structure of cell surface proteins, including BrkA-CBD, and prevented TAAK-A54 cells from binding to

chitin beads. Collectively, surface protein modifications mediated by OmpT and cell-surface protein antigens could have possibly introduced the inability to obtain significant results when the experiment was done in triplicates (Fig. 4S).

Nonetheless, we observed interactions between CBD-expressing cells and chitin beads (Fig. 3C). To ensure that the TAAK-A54 cells were actually interacting with the chitin beads, we washed the chitin beads after the 15-hour incubation two extra times and re-examined them. Even after these washes, the TAAK-A54 cells remained bound to the beads, suggesting an interaction facilitated by the CBD. These images reveal stained cells concentrated around the circumference of the bead (Fig. 3C) and dispersed along the bead surface. The limitation of the depth of focus of the light microscope may have prevented us from capturing the entire spherical surface of the chitin beads in a single focal plane. Although our observations suggested that chitin beads were covered with CBD-expressing cells, representative images could not be obtained due to microscope limitations.

Limitations One issue that arose was obtaining accurate results with the spectrophotometer due to fluctuating OD_{600} readings. To combat this problem, we increased the culture volume so that the laser could pass through our samples better and measured at multiple incubation time points, but the issue was not resolved. For improved accuracy in obtaining OD_{600} readings, future researchers can compare OD_{600} by fractionation. Fractions of cultures incubated with washed chitin resin can be extracted in equal amounts from top to bottom and transferred to a 96-well plate for OD_{600} measurements. This method is based on subcellular fractionation but uses gravity and time rather than separation based on molecular identity or centrifugation (26). Furthermore, the chitin assay experiments can be improved by transforming plasmids to UT5600 *E. coli* strain, which lacks outer membrane proteases such as OmpT and OmpP (23). Research suggests that the outer membrane proteases could lead to proteolysis of genetically modified passenger domains (14). Thus, the UT5600 strain may help maintain the cell-surface expression of BrkA-CBD. Due to inventory limitations, we were only able to access dyes to visualize the interaction between CBD-expressing cells and chitin. As Purple Violet dye is basic, this may introduce external factors that alter the interaction between CBD and chitin. An alternative way of visualizing CBD-expressing cell distribution on the surface of chitin beads is to co-transform bacterial cells with TAAK-A54 and a GFP-marker to facilitate fluorescence microscopy examination. This is a more gentle treatment on cells and may provide more stable environments for consistent interactions over time. Lastly, we were limited to using brightfield microscopy to visualize whole-cell immobilization. To capture more detailed images of chitin beads covered with CBD-expressing cells, scanning electron microscopy may be another option.

Conclusions In this study, a BrkA-6XHis-CBD recombinant plasmid (TAAK-A54) was designed via Gibson assembly to investigate the export of CBD protein via the BrkA autotransporter and the chitin-binding ability of CBD-expressing cells. Western blot analysis confirmed the presence of an expected intracellular CBD band at 52 kDa and an unexpected extracellular CBD at 38 kDa. Subsequent OD_{600} functional assays and microscopic examinations demonstrated the affinity of CBD-expressing cells for chitin, evident from their ability to bind and be pulled down by chitin. The results observed in cell immobilization through the BrkA autotransporter for CBD protein export preliminarily suggest the possibility of immobilizing other bacteria of interest or exporting various other proteins. Further tests should be conducted to justify the dose-dependency of the OD_{600} readings of TAAK-A54.

Future Directions In a broader context, bacteria immobilization can have an important role in water treatment and fermentation bioreactors. In untreated water, bacteria can utilize organic and inorganic matter as growth substrates. This enhances biological stability and lowers levels of micropollutants in water (25). One example is the removal of heavy metals by biosorption which can effectively remove a variety of heavy metals from aqueous solutions (26). If CBD is exported to the cell surface successfully in the correct conformation, chitin can be used to immobilize contaminated cells through its interaction with CBD. Bacteria adsorb to metals via the electrostatic and chemical association of metals with the organic functional groups on their cell surfaces (27). As a result, contaminated bacterial cells can be

removed from water using chitin. Since chitin binding is reversible, the same batch of bacteria can be reused to reduce cost and waste production. In fermentation bioreactors, immobilized cell systems have performance advantages over freely suspended cultures due to easy separation of biomass from the liquid and easy product recovery. The interaction of protein exported with type V secretion system and chitin provides a simpler way to immobilize cells, which offers an alternative to the current immobilization methods of non-specific adsorption and entrapment (28).

ACKNOWLEDGEMENTS

We would like to acknowledge Dr. David Oliver, whose guidance, support, and troubleshooting help were essential in completing this project and manuscript. We would like to thank Jade Muileboom for ordering and organizing materials, as well as for all her help in the lab. We would also like to thank Tatiana Lau for providing excellent inspiration and troubleshooting guidance. We would like to express our gratitude to the Department of Microbiology and Immunology at the University of British Columbia for funding this project and providing us with the lab space. We would also like to thank the anonymous reviewer for constructive feedback on this manuscript.

CONTRIBUTIONS

TW took the lead in Gibson assembly, verifying the recombinant plasmid, and testing CBD expression and export. AL took the lead in plasmid design and visualization of the interaction between CBD-expressing cells to chitin beads. KY took the lead in verifying the recombinant plasmid, and the OD functional assay. AZ assisted in testing CBD expression and export.

REFERENCES

1. **Lapponi MJ, Mendez MB, Trelles JA, Rivero CW.** 2022. Cell immobilization strategies for biotransformations https://doi.org/10.1016/j.cogsc.2021.100565.
2. **Wang J-Y, Chao Y-P.** 2006. Immobilization of Cells with Surface-Displayed Chitin-Binding Domain. Appl Environ Microbiol **72**:927–931.
3. **Saleemuddin M.** 1999. Bioaffinity based immobilization of enzymes. Adv Biochem Eng Biotechnol **64**:203–226.
4. **Rocha M, Yap M, Yoon M.** 2022. Expression of *Pseudomonas aeruginosa* PAO1 Chitinase C in Escherichia coli BL21 (DE3). Undergrad J Exp Microbiol Immunol **27**.
5. **Akagi K, Watanabe J, Hara M, Kezuka Y, Chikaishi E, Yamaguchi T, Akutsu H, Nonaka T, Watanabe T, Ikegami T.** 2006. Identification of the substrate interaction region of the chitin-binding domain of *Streptomyces griseus* chitinase C. J Biochem (Tokyo) **139**:483–493.
6. **Chern J-T, Chao Y-P.** 2005. Chitin-binding domain based immobilization of D-hydantoinase. J Biotechnol **117**:267–275.
7. **Alnadari F, Xue Y, Zhou L, Hamed YS, Taha M, Foda MF.** 2020. Immobilization of β-Glucosidase from Thermatoga maritima on Chitin-functionalized Magnetic Nanoparticle via a Novel Thermostable Chitin-binding Domain. Sci Rep **10**:1663.
8. **Pham M-L, Leister T, Nguyen HA, Do B-C, Pham A-T, Haltrich D, Yamabhai M, Nguyen T-H, Nguyen T-T.** 2017. Immobilization of β-Galactosidases from Lactobacillus on Chitin Using a Chitin-Binding Domain. J Agric Food Chem **65**:2965–2976.
9. **Simşek Ö, Sabanoğlu S, Çon AH, Karasu N, Akçelik M, Saris PEJ.** 2013. Immobilization of nisin producer *Lactococcus lactis* strains to chitin with surface-displayed chitin-binding domain. Appl Microbiol Biotechnol **97**:4577–4587.
10. **Rutherford N, Mourez M.** 2006. Surface display of proteins by Gram-negative bacterial autotransporters. Microb Cell Factories **5**:22.
11. **Fernandez RC, Weiss AA.** 1994. Cloning and sequencing of a *Bordetella pertussis* serum resistance locus. Infect Immun **62**:4727–4738.
12. **Oliver DC, Huang G, Fernandez RC.** 2003. Identification of Secretion Determinants of the *Bordetella pertussis* BrkA Autotransporter. J Bacteriol **185**:489–495.
13. **Sun F, Pang X, Xie T, Zhai Y, Wang G, Sun F.** 2015. BrkAutoDisplay: functional display of multiple exogenous proteins on the surface of *Escherichia coli* by using BrkA autotransporter. Microb Cell Factories **14**:129.
14. **Oliver DC, Huang G, Nodel E, Pleasance S, Fernandez RC.** 2003. A conserved region within the *Bordetella pertussis* autotransporter BrkA is necessary for folding of its passenger domain. Mol Microbiol **47**:1367–1383.

15. **Silacci M, Baenziger-Tobler N, Lembke W, Zha W, Batey S, Bertschinger J, Grabulovski D.** 2014. Linker Length Matters, Fynomer-Fc Fusion with an Optimized Linker Displaying Picomolar IL-17A Inhibition Potency. J Biol Chem **289**:14392–14398.
16. **Klemm P, Hjerrild L, Gjermansen M, Schembri MA.** 2004. Structure-function analysis of the self-recognizing Antigen 43 autotransporter protein from *Escherichia coli*. Mol Microbiol **51**:283–296.
17. **Feoktistova M, Geserick P, Leverkus M.** 2016. Crystal Violet Assay for Determining Viability of Cultured Cells. Cold Spring Harb Protoc **2016**:pdb.prot087379.
18. **Leo JC, Grin I, Linke D.** 2012. Type V secretion: mechanism(s) of autotransport through the bacterial outer membrane. Philos Trans R Soc B Biol Sci **367**:1088–1101.
19. **Folders J, Algra J, Roelofs MS, van Loon LC, Tommassen J, Bitter W.** 2001. Characterization of Pseudomonas aeruginosa chitinase, a gradually secreted protein. J Bacteriol **183**:7044–7052.
20. **Heissel S, Frederiksen SJ, Bunkenborg J, Højrup P.** 2019. Enhanced trypsin on a budget: Stabilization, purification and high-temperature application of inexpensive commercial trypsin for proteomics applications. PLOS ONE **14**:e0218374.
21. **Mahmood T, Yang P-C.** 2012. Western Blot: Technique, Theory, and Trouble Shooting. North Am J Med Sci **4**:429–434.
22. **Kirkland TN, Finley F, Orsborn KI, Galgiani JN.** 1998. Evaluation of the Proline-Rich Antigen of Coccidioides immitis as a Vaccine Candidate in Mice. Infect Immun **66**:3519–3522.
23. **Baneyx F, Georgiou G.** 1990. In vivo degradation of secreted fusion proteins by the *Escherichia coli* outer membrane protease OmpT. J Bacteriol **172**:491–494.
24. **Koga T, Asakawa H, Okahashi N, Takahashi I.** 1989. Effect of subculturing on expression of a cell-surface protein antigen by *Streptococcus mutans*. J Gen Microbiol **135**:3199–3207.
25. **Li Q, Yu S, Li L, Liu G, Gu Z, Liu M, Liu Z, Ye Y, Xia Q, Ren L.** 2017. Microbial Communities Shaped by Treatment Processes in a Drinking Water Treatment Plant and Their Contribution and Threat to Drinking Water Safety. Front Microbiol **8**:2465.
26. **Pham VHT, Kim J, Chang S, Chung W.** 2022. Bacterial Biosorbents, an Efficient Heavy Metals Green Clean-Up Strategy: Prospects, Challenges, and Opportunities. Microorganisms **10**:610.
27. **Konhauser KO, Fowle DA.** 2011. Microbial-Metal Binding, p. 654–657. *In* Reitner, J, Thiel, V (eds.), Encyclopedia of Geobiology. Springer Netherlands, Dordrecht.
28. **Zhu Y.** 2007. Chapter 14 - Immobilized Cell Fermentation for Production of Chemicals and Fuels, p. 373–396. *In* Yang, S-T (ed.), Bioprocessing for Value-Added Products from Renewable Resources. Elsevier, Amsterdam.